Preparation and Characterization of Chromium Doped Titania Hollow Nano-spheres

M. Ramezani*
Chemistry Department, North Tehran Branch, Azad University, Tehran, Iran,
H.R. Aghabozorg
Research Institute of Petroleum Industry, Tehran, Iran
F. Sakhaie
Chemistry Department, North Tehran Branch, Azad University, Tehran, Iran,

Abstract

Introduction: Hollow titania nanospheres have attracted much attention due to their wide applications in many fields, such as adsorption, catalysis and photocatalysis. Doping of different transition metals has enhanced photocatalytic properties of TiO_2.

Aim: Syntheses and characterization of Cr doped titania hollow nanospheres using sol-gel method and without template (for the first time).

Experimental: Hollow titania nanospheres synthesized by a simple sol-gel method and calcined in different temperatures. Then the prepared samples were characterized with X-ray diffraction (XRD), scanning electron microscopy (SEM) and transmission electron microscopy (TEM).

Results: The XRD patterns of samples show that the maximum mole fraction of Cr doping level in TiO_2 is around 30% and the crystal lattice parameter decreases with Cr doping. Pure TiO_2 and Cr doped TiO_2 calcined at 500 °C both are in anatase phase but for pure TiO_2 with increasing calcination temperature rutile phase starts to appear. The fraction of the rutile phase is greatly reduced for Cr doped TiO_2 hollow spheres in comparison with pure TiO_2 hollow spheres at 700 °C. The SEM and TEM images indicate that the prepared samples are spherical. The mean diameters of the spheres are estimated using the Scherrer equation. The size of the crystal grains of the TiO_2 hollow spheres increases with increasing calcination temperature and decreases with increasing calcination time.

Conclusion: The maximum mole fraction of Cr doping in hollow titania spheres is around 30%. For pure TiO_2 with increasing calcination temperature rutile phase starts to appear. The fraction of the rutile phase is greatly reduced for Cr doped TiO_2 hollow spheres at 700 °C. The crystal lattice parameters calculated from the XRD patterns of the prepared samples show that the crystal lattice parameter (c) of the samples decreases with Cr doping.

Keywords: Hollow nano-sphere, Chromium doped titania, Sol-gel method, Rutile and anatase phase.

*Corresponding autour

Introduction

Hollow nanospheres of inorganic materials have attracted much attention due to their wide applications in many fields, which include controlling storage and release, adsorption, using as fillers and catalysts.[1-3] There are various methods for the fabrication of hollow spheres such as template-assisted process including polystyrene latex particles or silica particles and their crystalline arrays, emulsion polymer micelles, hydrothermal and ultrasonication. [4-9] Titanium dioxide crystallizes in different structures such as rutile, anatase and brookite. TiO_2 has been widely applied in many fields such as antibacterial actions [10], catalysis and photocatalysis. [11-13] TiO_2 displays its high photoactivity only when it is irradiated by ultraviolet light due to its wide band gap (3.2 ev for anatase phase). It is of great interest to employ visible region, where less expensive light sources exist, to activate TiO_2 for photocatalyic aims. An effective way to enhance photocatalytic properties is doping different transition metal ions such as Co, V, Fe, Ce and Cr into TiO_2 powder. [14-20] Shah et al. [21] successfully used the metallorganic chemical vapor deposition method to synthesize pure TiO_2 and Pd(II), Pt(IV) and Fe(III) doped TiO_2 nanoparticles. The photocatalytic efficiency was remarkably enhanced by the introduction of Pd(II). However, Pt(IV) changed the 2-chlorophenol degradation rate only slightly, and Fe(III) was detrimental to this process. Yu et al. [22] have found that Sn substitution for Ti in rutile TiO_2 increased the photoactivity of the rutile phase in the oxidation of acetone. Sibu et al. [23] included La_2O_3 into nanosized TiO_2 by the sol-gel method. They found that the surface area of titanium oxide was increased from about 1 to 52 m^2/g when 1% La_2O_3 was present. Mitadera and Hinode [24] prepared Nb/TiO_2 using the impregnation method and found that Nb/TiO_2 catalyst showed high activity and selectivity in the reduction of NO to N_2. The maximum conversion of NO to N_2 was reached with the composition of Nb (10 wt%)/TiO_2. Cr seems to be one of the most promising dopant in TiO_2 as it improves the photocurrent density of TiO_2. [25-27] Lee et al. [26] prepared Cr/Ti hollow spheres using poly-(styrene-methyl acrylic acid) latex particles as a template. They found that the fabricated TiO_2 hollow spheres (with/without Cr) exhibit considerable levels of MB photocomposition (>35%) within just 3h of visible light irradiation. 0.5% Cr/Ti hollow sphere showed the highest MB photodecomposition under visible light. The presence of Cr(III) enhanced the light absorption of the specimens in the visible region hindering the TiO_2 phase transformation to a rutile phase resulting in improved MB decomposition. Lu et al. [28] synthesized Cr doped TiO_2 thin films by cathodic arc plasma evaporation on silicon wafers. In this work, titania hollow nanospheres doped with chromium were prepared by the sol-gel method and without template. The prepared samples were characterized with X-ray diffraction (XRD), scanning electron microscopy (SEM) and transmission electron microscopy (TEM).

Experimental

The stoichiometric amount of $Cr(NO_3)_3.9H_2O$ (98% Panreac) was first dissolved in 20 ml absolute ethanol and 1ml distilled water, then 0.00075 mol citric acid was added to this solution. 5 ml of $NH_3.H_2O$ (25% Merck) was added to above solution. Finally, the stoichiometric amount of titanium butoxide (98% Merck) and another 5 ml ammonia were dripped to the above solution simultaneously. The mixed solution was left to stand for 2h. Then the precipitate was filtered, washed with distilled water and ethanol followed by drying at 60 °C for 7h.

Powder XRD patterns were obtained on Rigaku D/Max γA X-ray diffractometer with Cu Kα radiation (λ =1.54056 Å). SEM (SEM Philips XL 30, Germany) and TEM (Philips EM 208, Germany) were used to investigate the morphology of the samples. The mean diameters of the spheres were calculated using the Scherrer equation: $\beta = 0.89\lambda/D\cos\theta_{max}$, where β is the

angular width at the half maximum intensity of the diffraction line for the sample, λ = wavelength of radiation, D = average anatase grain size, θ = diffraction angle of the crystal plane (hkl).

Results and discussion

The XRD patterns of pure TiO_2 calcined at different temperatures are shown in figure 1. It can be seen that the samples have anatase phase in lower temperatures and with increasing temperature the rutile phase starts to appear (All the relatively sharp picks of the XRD patterns of the synthesized samples are compared with the standard samples indexed as JCPDS[1] 21-1272 and 21-1276). Thus, 500 °C is chosen as the favorite calcination temperature in this experiment. The effect of calcination time on the phase transformation (from anatase to rutile), is studied at 700 °C (figure 2). The XRD patterns show that by increasing the calcination time, phase transformation increases. Figure 3 shows the XRD patterns of Cr doped TiO_2 powder calcined at 500 °C with different Cr contents. In comparison with the XRD patterns of pure TiO_2, It is found that Cr doped TiO_2 spheres have anatase structure after calcination at 500 °C for 4h. For the sample with 40% Cr content, another phase has appeared. Therefore, the maximum mole fraction of Cr is around 30%. Figure 4 shows the XRD patterns of pure TiO_2 (a) and 30% Cr doped TiO_2 (b) calcined at 700 °C. At this temperature, the fraction of the rutile phase is greatly reduced for Cr doped TiO_2 hollow spheres in comparison with pure TiO_2 hollow spheres. It shows that Cr doping hinders the phase transformation from anatase into rutile phase during the calcination process.

Figures 5 and 6 show the typical SEM and TEM images of the synthesized hollow spheres. These images indicate that the prepared samples are spherical. The mean diameter of the spheres is estimated using the Scherrer equation. The results are given in tables 1-3. The size of the crystal grains of the TiO_2 hollow spheres increases with increasing calcination temperature and decreases with increasing calcination time (table 1 and 2). According to figure 2 by increasing the calcination time, phase transformation increases. This result is reasonable and can be due to the unit cell volume of the rutile phase (62.43 $Å^3$) which is less than that of anatase phase (136.31 $Å^3$). The mean grain diameter of the TiO_2 hollow spheres increases by the Cr doping (table 3). Table 4 summarizes the crystal lattice parameters calculated from the XRD patterns for the pure TiO_2 samples and 30% Cr doped TiO_2. This table shows that the crystal lattice parameter (c) of the samples decreases with Cr doping.

1- Joint Committee on Powder Diffraction Standard

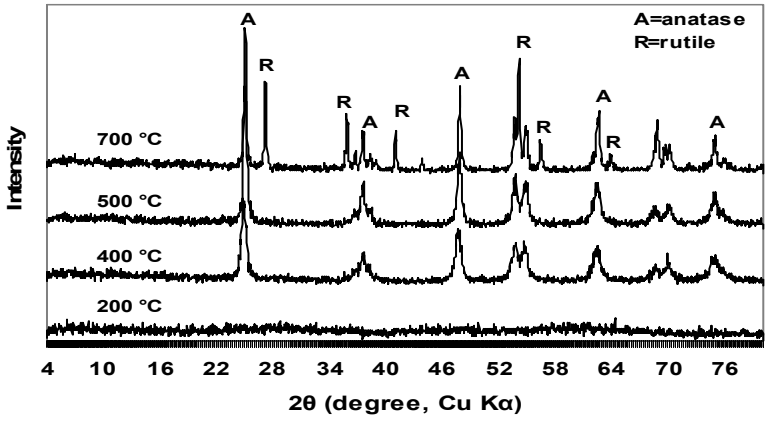

Fig. 1- XRD patterns of pure TiO_2 calcined at different temperatures (intensive peaks of anatase and rutile phases are indicated)

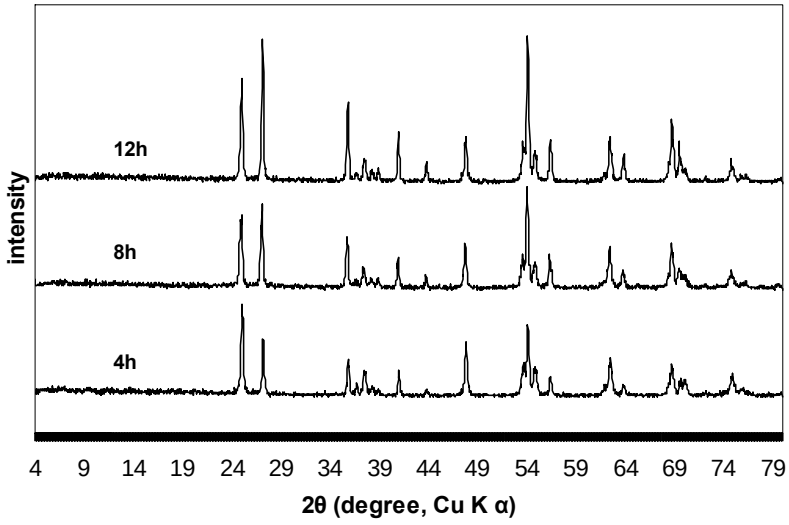

Fig. 2- XRD patterns of pure TiO_2 calcined at 700 °C and different calcination times

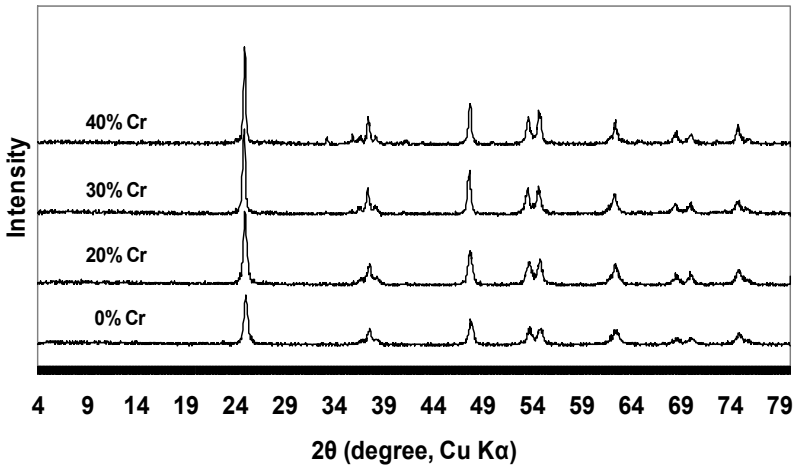

Fig. 3- XRD patterns of Cr doped TiO_2 calcined at 500 °C with different Cr contents

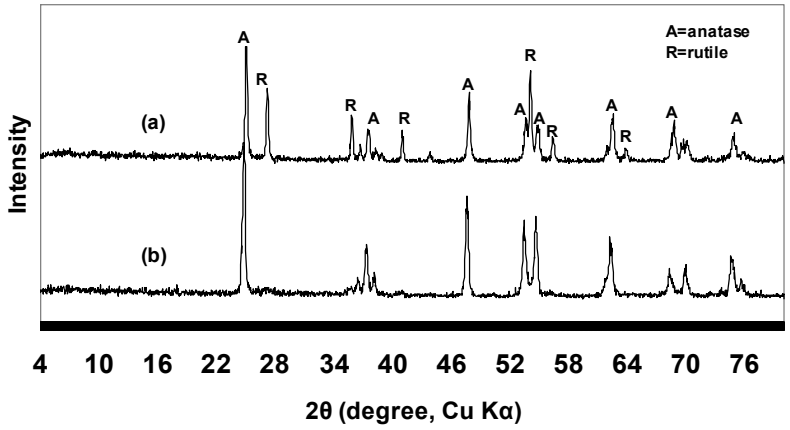

Fig. 4- The XRD patterns of pure TiO_2 (a) and 30% Cr doped TiO_2 (b) calcined at 700 °C

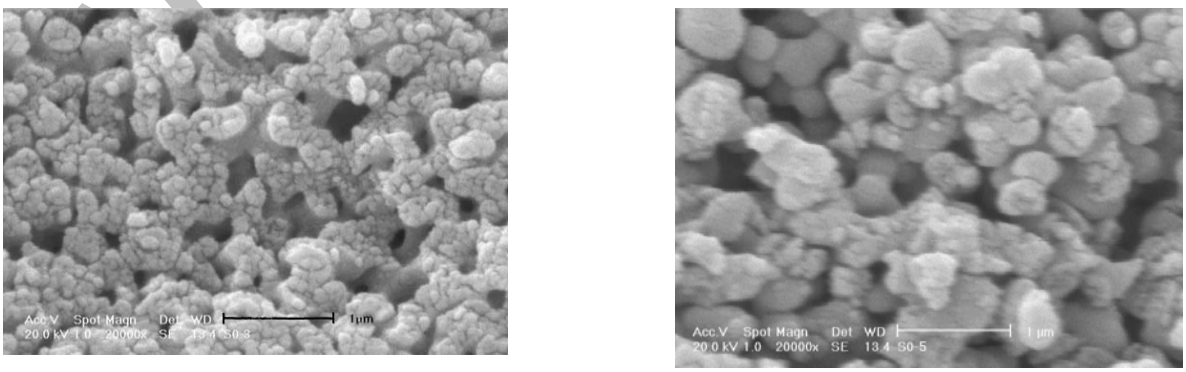

(a) ***(b)***

Fig. 5- The SEM images of pure titania spheres (a) and Cr doped titania spheres (b)

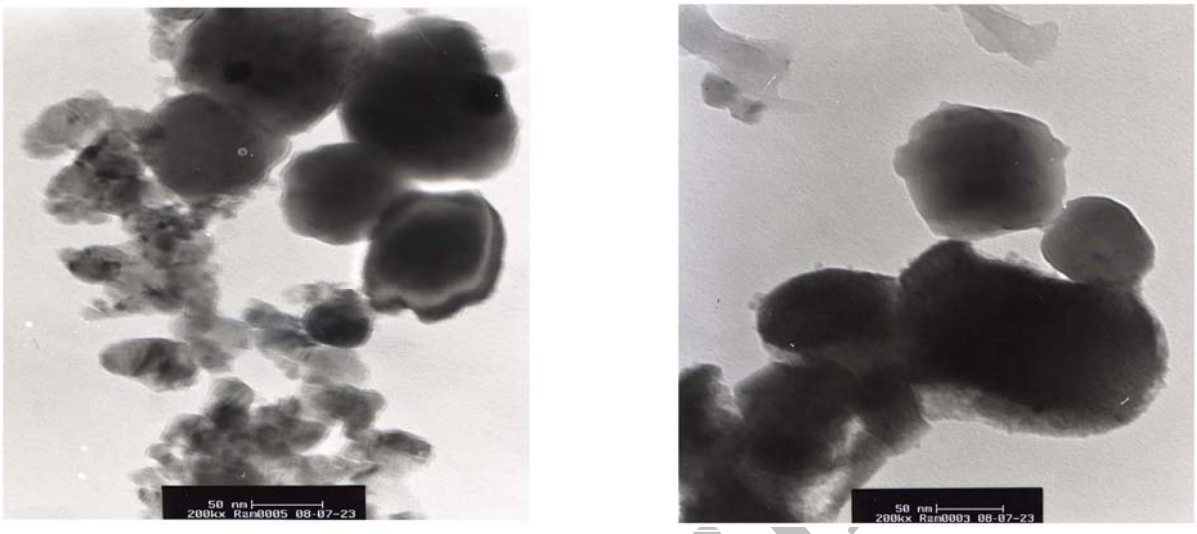

(a) ***(b)***

Fig. 6 -The TEM images of pure titania spheres (a) and Cr doped titania spheres (b).

Table 1- Grain size of pure TiO_2 prepared at different temperatures

Calcination temperature (°C)	400	50	70
Pure TiO_2 grain size (nm)	21	29	48

Table 2- Grain size of pure TiO_2 calcined at 700 °C and different calcination times

Calcination time (h)	4	8	12
Pure TiO_2 grain size (nm)	48	42	37

Table 3- The grain size of Cr doped TiO_2 prepared at 500 °C

Cr content (mol. %)	10	20	30
Grain size (nm)	29	32	40

Table 4- The crystal lattice parameters of pure TiO_2 and Cr doped TiO_2

Cr	a (nm)	c (nm)
0	3.789	9.775
0.15	3.789	9.450

Conclusions

Hollow titania spheres doped with Cr were successfully synthesized with a simple sol-gel method without using template for the first time in this work. XRD patterns of the synthesized samples showed that pure TiO_2 and Cr doped TiO_2 calcined at 500 °C both were in the anatase phase. These patterns showed that the maximum mole fraction of Cr doping in hollow titania spheres was around 30%. For pure TiO_2 with increasing calcinations temperature rutile phase started to appear. The fraction of the rutile phase was greatly reduced for Cr doped TiO_2 hollow spheres in comparison with pure TiO_2 hollow spheres at 700 °C. The crystal lattice parameters calculated from the XRD patterns of the prepared samples showed that the crystal lattice parameter (c) of the samples decreased with Cr doping.

References:

1. Rengarajan, R., Jiang, P., Colvin, V., and Mittleman, D., *Appl. Phys. Lett*., **77**, 3517 (2000).
2. Huang, H., and Remsen, E.E., *J. Am. Chem. Soc*., **121,** 3805 (1999).
3. Kim, S.W., Kim, M., Lee, W.Y., and Hyeon, T., *J. Am. Chem. Soc*., **124**, 764 (2002).
4. Li, G. C., and Zhang, Z. K., *Material letter*, **58**, 2768 (2004).
5. Zhong, Z., Yin, Y., Gates, B., and Xia, Y., *Adv. Mater*., **12,** 206 (2000).
6. Shiho, H., and Kawahashi, N., *Colloid Polym. Sci*., **278**, 270 (2000).
7. Stefanie, E., and Georg, M., *J. Colloid Interface Sci*., **250**, 281 (2002).
8. Fujikawa, S., and Kunitake, T., *Chem. Lett.*, 1134 (2002).
9. Wijnhoven, J.E.G.J., and Vos, W.L., *Science*, **281,** 802 (1998).
10. Kartsonakis, I.A., Liatsi, P., Danilidis, I., Bouzarelou, D., and Kordas, G., *J. Phys. Chem of solid*, **69**, 214 (2008).
11. Schattka, J.H., Shchukin, D.G., Jia, J., Antonietti, M., and Caruso, R.A., *Chem.Mater*., **14,** 5103 (2002).
12. Lei, Z., Li, J., Ke, Y., Zhang, Y., Zhang, H., and Li, F., *J. Mater. Chem*., **11**, 2930 (2001).
13. Goutailler, G., Guillard, C., Daniele, S., and Pfalzgraf, L.G.H., *J. Mater. Chem*., **13**, 342 (2003).
14. Caimei, F., Peng, X., and Yanping, S., *journal of rare earths*, **24**, 309 (2006).
15. Jimmy, C.Y., Jun, L., and Raymund, W.M.K., *Journal of Rare Earths*, **22**, 591 (2004).
16. Liang, J., Jin, Z., and Wang, J., *Journal of the Chinese of Ceramic Society*, **29**, 500 (2001).
17. Yamashita, H., Harada, M., and Misaka, J., *J. Photochem. Photobiol*, **148**, 257 (2002).
18. Choi, W**.,** Termin, A., and Hoffmann, M.R., *J. Phys. Chem*., **98,** 13669 (1994).
19. Chao, H.E., Yun, Y.U., and Xing F., *Journal of European Ceramic Society*, **23**, 1457 (2003).
20. Yuan, Z., Jia, J., and Zhang, L., *Materials Chemistry and Physics*, **73**, 323 (2002).
21. Shah, S.I., Li, W., Huang, C.P., Jung, O., and Ni, C., *Proc. Natl Acad. Sci*. USA, **99**, 6482 (2002).
22. Lin, J., Yu, J.C., Lo, D., and Lam, S.K., *J. Catal*., **183**, 368 (1999).
23. Sibu, C.P., Kumar, S.R., Mukundan, P., and Warrier, K.G.K., *Chem. Mater*., **14**, 2876 (2002).
24. Mitadera, J., and Hinode, H., *Appl. Catal. B: Environ*., **39**, 205 (2002).
25. Zhu, J., Deng, Z., Chen, F., Zhang, J., Chen, H., Anpo, M., Huang, J., and Zhang, L.,

Appl. Catal. B. Environ., **62**, 329 (2006).
26. Kim, H.R., Eom, Y., Lee, T.G., and Shul, Y.G., *Mater. Phys. Chem*., **108**, 154 (2008).
27. Radecka, M., Wierzbicka, M., Komornicki, S., and Rekas, M., *Phys. B*., **348**, 160 (2004).
28. Chan, M.H., Ho, W.Y., Wang, DS.Y., and Lu, F.H., *Surface & Coatings Technology*, **202**, 962 (2007).